HIV-1 Tat and opioids act independently to limit antiretroviral brain concentrations and reduce blood–brain barrier integrity

Crystal R. Leibrand[1] · Jason J. Paris[2] · Austin M. Jones[1] · Quamrun N. Masuda[3] · Matthew S. Halquist[3] · Woong-Ki Kim[4] · Pamela E. Knapp[5,6,7] · Angela D. M. Kashuba[8] · Kurt F. Hauser[5,6,7] · MaryPeace McRae[1]

Abstract

Poor antiretroviral penetration may contribute to human immunodeficiency virus (HIV) persistence within the brain and to neurocognitive deficits in opiate abusers. To investigate this problem, HIV-1 Tat protein and morphine effects on blood–brain barrier (BBB) permeability and drug brain penetration were explored using a conditional HIV-1 Tat transgenic mouse model. Tat and morphine effects on the leakage of fluorescently labeled dextrans (10-, 40-, and 70-kDa) into the brain were assessed. To evaluate effects on antiretroviral brain penetration, Tat+ and Tat− mice received three antiretroviral drugs (dolutegravir, abacavir, and lamivudine) with or without concurrent morphine exposure. Antiretroviral and morphine brain and plasma concentrations were determined by LC-MS/MS. Morphine exposure, and, to a lesser extent, Tat, significantly increased tracer leakage from the vasculature into the brain. Despite enhanced BBB breakdown evidenced by increased tracer leakiness, morphine exposure led to significantly lower abacavir concentrations within the striatum and significantly less dolutegravir within the hippocampus and striatum (normalized to plasma). P-glycoprotein, an efflux transporter for which these drugs are substrates, expression and function were significantly increased in the brains of morphine-exposed mice compared to mice not exposed to morphine. These findings were consistent with lower antiretroviral concentrations in brain tissues examined. Lamivudine concentrations were unaffected by Tat or morphine exposure. Collectively, our investigations indicate that Tat and morphine differentially alter BBB integrity. Morphine decreased brain concentrations of specific antiretroviral drugs, perhaps via increased expression of the drug efflux transporter, P-glycoprotein.

Keywords Dolutegravir · Abacavir · Lamivudine · Neuro-human immunodeficiency virus (neuroHIV) · P-glycoprotein · Zonula occludens-1 · Morphine-3-β-glucuronide · Transcellular transport · Paracellular transport

Introduction

Despite the aggressive use of combination antiretroviral therapy (cART), HIV infection in the nervous system (neuroHIV) results in neurocognitive and neurobehavioral impairment in about half of infected individuals (Sacktor et al. 2002; Ellis et al. 2007; Tozzi et al. 2007; Cysique and Brew 2009). Although the severity has diminished in the post-cART era, HIV-associated neurocognitive disorders (HAND) persist as HIV/AIDS evolves into a chronic disease (Ellis et al. 2007;

✉ MaryPeace McRae
mpmcrae@vcu.edu

1 Department of Pharmacotherapy and Outcomes Science, School of Pharmacy, Virginia Commonwealth University, Richmond, VA 23298, USA

2 Department of BioMolecular Sciences, School of Pharmacy, The University of Mississippi, University, MS 38677, USA

3 Department of Pharmaceutics, School of Pharmacy, Virginia Commonwealth University, Richmond, VA 23298, USA

4 Department of Microbiology and Molecular Cell Biology, Eastern Virginia Medical School, Norfolk, VA 23507, USA

5 Department of Pharmacology and Toxicology, School of Medicine, Virginia Commonwealth University, Richmond, VA 23298, USA

6 Department of Anatomy and Neurobiology, School of Medicine, Virginia Commonwealth University, Richmond, VA 23298, USA

7 Institute for Drug and Alcohol Studies, Virginia Commonwealth University, Richmond, VA 23298, USA

8 Division of Pharmacotherapy and Experimental Therapeutics, Eshelman School of Pharmacy, University of North Carolina at Chapel Hill, Chapel Hill, NC 27599-7569, USA

Vivithanaporn et al. 2011). Poor central nervous system (CNS) penetration of antiretroviral drugs likely contributes to HIV persistence and chronic inflammation within the brain, despite the fact that viral loads are often reduced to non-detectable levels in peripheral circulation.

Opiate drug abuse can exacerbate the cognitive impairment and pathologic CNS changes in HIV-infected persons. HIV neuropathogenesis and cognitive deficits are exacerbated with opiate co-exposure (Donahoe and Vlahov 1998; Hauser et al. 2007), potentiating HIV replication (Peterson et al. 1990, 1993, 1994; Li et al. 2002; Nath et al. 2002; Kumar et al. 2006), glial activation (El-Hage et al. 2005, 2006, 2008; Turchan-Cholewo et al. 2009; Zou et al. 2011), neurotoxicity (Gurwell et al. 2001; Fitting et al. 2010a, 2014), and blood–brain barrier (BBB) breakdown (Mahajan et al. 2008; Dutta and Roy 2012). Despite HIV and drug abuse being inextricably linked, morphine- and HIV-interactive effects on the actual penetration of therapeutic drugs into the brain are not well studied.

The BBB is a selective barrier, limiting passage of substances from blood into the brain. The BBB is composed of microvascular endothelial cells lining brain microvessels that are surrounded by basal lamina, astrocytic perivascular endfeet, and pericytes, which contribute to the induction and maintenance of BBB properties (Janzer and Raff 1987; Dehouck et al. 1990; Hayashi et al. 1997; Dohgu et al. 2005; Abbott et al. 2006, 2010; Winger et al. 2014). Continuous tight junction (TJ) complexes restrict movement of water-soluble compounds between adjacent cells and force most molecular traffic to traverse via a transcellular route. Although small lipophilic molecules can freely diffuse through lipid membranes (Abbott et al. 2006), specific transport systems regulate transcellular traffic of small hydrophilic molecules, influencing uptake and efflux of compounds from the brain. These transporters can influence directional flux of xenobiotics. Examples of drug efflux proteins responsible for expulsion of substances from brain endothelial cell cytoplasm back into blood are P-glycoprotein (ABCB1), breast cancer resistance protein (BCRP, ABCG2), and select members of the multidrug resistance protein family (MRP, ABCC) (Wilhelm et al. 2011). Lastly, the BBB serves as an enzymatic barrier, composed of both intracellular and extracellular enzymes, capable of metabolizing and inactivating many chemical compounds (Abbott et al. 2006, 2010; Dauchy et al. 2009). The BBB permits maintenance of a unique extracellular microenvironment that is essential for normal CNS function.

The rate and extent to which a drug will cross the BBB and penetrate into the brain are influenced by the physicochemical properties of drugs, including lipophilicity, molecular weight, charge at physiologic pH, and protein binding (Abbott et al. 2010). Additionally, depending on the transporter(s) involved, active transport systems can facilitate or hinder brain penetration of drugs. Furthermore, BBB "breakdown," which classically refers to tight junction disruption and/or flux of paracellular compounds, does not necessarily predict changes in the flux of drugs that primarily traverse the BBB by transcellular (through the cells) or the net flux of drugs that traverse via multiple mechanisms (Gan et al. 1993; Troutman and Thakker 2003). Indeed, factors affecting transcellular permeability and paracellular permeability are thought to be independently regulated (Liebner et al. 2018).

HIV-derived cellular and viral toxins are known to alter the integrity of the BBB. Exposure to HIV alters tight junction expression (Dallasta et al. 1999; Boven et al. 2000; Persidsky et al. 2006; Chaudhuri et al. 2008a, b; Eugenin et al. 2011) and also increases transmigration of cells across the barrier (Saukkonen et al. 1997; Persidsky et al. 1999, 2000; Eugenin 2006; Buckner et al. 2011; Eugenin et al. 2011; Williams et al. 2012; Coley et al. 2015). The HIV proteins Tat (transactivator of transcription) and/or gp120 (glycoprotein 120) decrease tight junction protein expression (Kanmogne et al. 2002, 2007; Price et al. 2005; Shiu et al. 2007; Nakamuta et al. 2008; Louboutin et al. 2010; Louboutin and Strayer 2012), increase transmigration of monocytes (Weiss et al. 1999; Wu et al. 2000; Buckner et al. 2006, 2011; Williams et al. 2013, 2015), and increase barrier permeability to paracellular compounds (Andras et al. 2003; András et al. 2005; Pu et al. 2005, 2007; Zhong et al. 2008; Banerjee et al. 2010; Gandhi et al. 2010; Xu et al. 2012; Leibrand et al. 2017).

Morphine exposure has been reported to regulate the expression of tight junction proteins (Mahajan et al. 2008; Wen et al. 2011) and can alter transendothelial electrical resistance (TEER; a measure of barrier integrity) (Mahajan et al. 2008), although the findings of the effects of opiates on barrier permeability are inconsistent. The range of findings include claims that morphine exposure increases BBB permeability (a "leaky" barrier) (Wen et al. 2011), to those asserting there is no change in permeability (Yousif et al. 2008; Strazza et al. 2016), or even decreased permeability to paracellular markers, suggesting enhanced barrier function (Sharma and Ali 2006). While the mechanisms by which opiates effect the paracellular permeability of the BBB are uncertain, morphine has been shown to disrupt tight junctional complexes in columnar epithelium lining the small intestine (Meng et al. 2013). In the small intestine, morphine acts via a signaling pathway involving the upregulation of toll-like receptor 2 (TLR2) and toll-like receptor 4 (TLR4) and a myosin light chain kinase-dependent redistribution of the tight junctional proteins, zonula occludens-1 (ZO-1), and occludin (Meng et al. 2013). Besides having effects on paracellular transport, morphine exposure can also affect the expression of drug efflux transporters associated with transcellular transport through the

endothelial cell component of the BBB (Miller et al. 2008; Yousif et al. 2008; Mahajan et al. 2008). Thus, the nature of opiate-dependent reductions or improvements in barrier function likely result from independent actions on paracellular and transcellular processes and are likely subject to the timing and duration of exposure (Aquilante et al. 2000; Miller et al. 2008; Yousif et al. 2008; Mahajan et al. 2008).

The purpose of this study was to examine the effects of the HIV-1 protein Tat and morphine on antiretroviral penetration into the brain in concert with measurements of any alterations in the integrity of the BBB. We hypothesized that opiate abuse would exacerbate HIV-1 Tat-mediated BBB breakdown, but also that antiretroviral penetration into the brain would be limited by Tat and/or morphine exposure. Specifically, we examined the effects of Tat expression and morphine exposure on ARV concentrations within the striatum and hippocampus. There are regional differences in HIV viral loads within the brain; post-mortem studies have demonstrated that the basal ganglia and hippocampus are both associated with higher viral levels than cerebellar cortex or mid-frontal cortical gray matter (Fujimura et al. 1997; Wiley et al. 1998; Nath 2015). Furthermore, the dorsal striatum is particularly vulnerable to the effects of HIV (Nath 2015), and Tat-induced damage within the striatum is well characterized in the Tat transgenic mouse model (Bruce-Keller et al. 2008; Fitting et al. 2010b; Leibrand et al. 2017). In contrast, the hippocampus exhibits a more subtle pathology in response to Tat exposure. These changes include marked impairments to hippocampal function (reduces long-term potentiation in CA1 pyramidal neurons and deficits in learning/memory), despite only slight reductions in the density of CA1 pyramidal cell dendritic spines (Fitting et al. 2013). In the Tat transgenic and murine AIDS (MAIDS) models, there are regional differences in cytokine release in response to Tat exposure or viral infection and also to morphine exposure (Fitting et al. 2010b; McLane et al. 2018). To assess the effects of Tat and morphine on ARV concentrations within the striatum and hippocampus, mice that conditionally expressed HIV-1 Tat (Tat+) or their control counterparts (Tat−) were exposed to morphine or a placebo treatment. All mice received the antiretroviral drug combination dolutegravir/abacavir/lamivudine by continuous administration via an osmotic pump. After 5 days of antiretroviral drug exposure, brain and plasma were collected for quantification of antiretroviral drug concentrations. To determine the extent of BBB leakiness, mice were exposed to Tat, with or without morphine, and given transcardial injections of the labeled dextrans, Cascade Blue® (10 kDa), fluorescein (40 kDa), and Texas Red® (70 kDa).

Understanding how opioid abuse alters the penetration of antiretroviral drugs into the brain may lead to an improved understanding of why opioid abusers can exhibit more severe neurocognitive impairment and may lead to the development of better therapeutic drug regimens for neuroHIV.

Materials and methods

Subjects and housing

The use of mice in these studies was approved by the Institutional Animal Care and Use Committee at Virginia Commonwealth University, and the experiments were conducted in accordance with ethical guidelines defined by the National Institutes of Health (NIH Publication No. 85–23). Adult, female mice (approximately 70 days of age) were utilized for these initial studies given their capacity for a more dynamic neuroimmune response to a range of insults compared to adult males (Schwarz et al. 2012; Hanamsagar et al. 2017). Mice were generated in the vivarium at Virginia Commonwealth University and either expressed an HIV-1 *tat* transgene (Tat+) or were control counterparts that lacked the *tat* transgene (Tat−). Tat+ mice conditionally expressed the HIV-1 Tat$_{1-86}$ protein in a nervous system-targeted manner via a glial fibrillary acidic protein (GFAP)-driven, tetracycline (Tet)-on promoter, which was activated by consumption of chow containing doxycycline. Tat− controls expressed only the doxycycline-responsive reverse tetracycline-controlled transcription factor as previously described (Bruce-Keller et al. 2008; Hauser et al. 2009). All mice were placed on doxycycline-containing chow (Dox Diet #2018; 6 g/kg) obtained from Harlan Laboratories (Madison, WI) for the duration of Tat induction and then placed on regular feed. Mice were housed four to five per cage and were maintained in a temperature- and humidity-controlled room on a 12-h to 12-h light/dark cycle (lights off at 18:00 h) with ad libitum access to food and water.

Antiretroviral and morphine administration

Triumeq® (ViiV Healthcare) is a combination tablet containing abacavir (600 mg), dolutegravir (50 mg), and lamivudine (300 mg) and was purchased from the VCU Health Systems Pharmacy. The dosing for mice was calculated via allometric scaling (Nair and Jacob 2016), based on an average 20 g mouse and was as follows: abacavir 2.5 mg/day (123.5 mg/kg/day), dolutegravir 0.2 mg/day (10.3 mg/kg/day), and lamivudine 1.2 mg/day (61.7 mg/kg/day). In brief, tablets were crushed to a fine power and resuspended in normal saline. After centrifugation at 1000 rpm for 5 min to pellet tablet excipients, the supernatant was sterile filtered twice (0.45 μm followed by 0.22 μm filter). Following filtration, 210 μL was loaded into the ALZET® osmotic pump (Model 2001, 1 μl/h delivery). For morphine groups, morphine salt pentahydrate powder was diluted directly into the antiretroviral solution prior to loading into the pump at a concentration sufficient to deliver 2.0 mg/day. Drug preparations were made in batches to minimize dosing variability.

Morphine administration in dextran exclusion studies

For dextran exclusion studies, morphine or placebo administration was achieved by subcutaneous implantation of 25 mg morphine or placebo time-release pelleted implants (National Institute on Drug Abuse, NIDA, Drug Supply System, Rockville, MD) under aseptic conditions and 4% isoflurane anesthesia. The use of time-release morphine pelleted implants or tablets is a standard method to continuously administer morphine during a period of 5 to 7 days. The 25-mg pelleted implants produce morphine drug concentrations in the brain sufficient to cause tolerance (Chefer and Shippenberg 2009) and physical dependence (Bogulavsky et al. 2009) within 3 days in C57BL/6 mice, and these concentrations are comparable to plasma/tissue levels achieved in humans who are opiate-dependent (Ghazi-Khansari et al. 2006).

Briefly, mice were anesthetized with isoflurane (4% induction, 2% maintenance). A small mid-scapular entry was made through the skin and either a time-release 25-mg morphine or placebo pellet (dextran exclusion studies) or an ALZET® osmotic pump delivering 2.0 mg morphine/day or placebo (antiretroviral and morphine accumulation studies) was implanted. Bupivacaine was applied to all surgical sites immediately post-op. Sample sizes range from six to nine mice per group for dextran exclusion studies and antiretroviral accumulation studies.

Assessment of blood–brain barrier permeability

To assess the influence of HIV-1 Tat and morphine on BBB integrity, Tat+ and Tat− mice received doxycycline chow (to induce Tat expression, if applicable) for 14 days followed by a 5-day no-doxycycline washout period. At the conclusion of the 5-day washout period, Tat+ and Tat− mice were subcutaneously implanted with either morphine or placebo pellets. Five days after pellet implantation, mice were transcardially infused with either 10 mL of dextran solution in phosphate-buffered saline (PBS) containing 10 kDa dextrans conjugated to Cascade Blue® (0.1 mg/mL), 40 kDa dextrans conjugated to fluorescein (0.1 mg/mL), and 70 kDa dextrans conjugated to Texas Red® (0.1 mg/mL) over 5 min or with 10 μL ~44 kDa HRP (5 mg/mL; 5 min prior to perfusion with 15 mL PBS followed by 20 mL 4% paraformaldehyde) (Leibrand et al. 2017). BBB permeability was assessed via multiple methods: Na-F and Texas Red-labeled dextran were measured in brain homogenates, whereas HRP brain penetration was measured immunohistochemically in whole-brain sections. Brains were homogenized in a 10× volume of 50% trichloroacetic acid, centrifuged at 5000×g at 4 °C for 10 min, and then the supernatant was neutralized with 5 M NaOH (1:8 ratio) per prior methods (Ramirez et al. 2012; Leibrand et al. 2017). Cascade Blue, fluorescein, and Texas Red-labeled dextrans were measured via spectrophotometry (Cascade Blue®-dextrans: 380/460 nm, ex/em; fluorescein-dextrans: 485/520 nm, ex/em; and Texas Red®-dextrans: 575/620 nm, ex/em) using a PHERAStar FS Plus microplate reader (BMG Labtech) on glass-bottom multi-well cell culture plates. Dextran data were expressed as fold change in fluorescent intensity/well (500 μL volume) compared to Tat− placebo-pelleted control mice (Hawkins and Egleton 2006; Leibrand et al. 2017). For HRP experiments, frozen coronal slices (40 μm-thick) were labeled with primary anti-HRP and visualized via appropriate secondary antibody conjugated to Alexa Fluor 647 (Alexa 647, Thermo Fisher, Rockford, IL; *far-red fluorescence*) as previously described (Leibrand et al. 2017). Briefly, slices were counterstained with Hoechst 33342 nuclear stain (Thermo Fisher; *blue fluorescence*) and imaged as described (Marks et al. 2016; Leibrand et al. 2017). HRP signal was normalized to background (signal intensity in the off-tissue area of the tiled image). HRP signal above background levels indicates BBB disruption and leakage of HRP into the brain (Ben-Zvi et al. 2014). Tiled images of HRP and Hoechst dual-labeled sections in the dorsal striatum were acquired from within a single z-plane (~ 0.50 μm-depth) within 5 μm from the surface of the section. HRP immunofluorescence was detected in the far-red range (Alexa 647) using diode laser excitation (637 nm) with a 640-nm long-pass filter. All images were acquired using a Zeiss LSM700 confocal microscope (Oberkochen, Germany) equipped with a 20 × 1.0 NA objective. During image acquisition, the laser intensity, detector gain, and all other parameters were held constant within an identical volume of tissue across all treatment groups.

Antiretroviral accumulation in dorsal striatum and hippocampus

To assess the effects of HIV-1 Tat and morphine on antiretroviral accumulation in the dorsal striatum and hippocampus, Tat+ and Tat− mice received doxycycline chow (for Tat induction) for 14 days followed by a 5-day period in which doxycycline was not administered to clear the antibiotic from the system. Prior (Ngwainmbi et al. 2014) and unpublished studies indicate that Tat mRNA expression remains elevated (including that detected in striatum and hippocampus) for at least 3 weeks after withholding doxycycline. On day 5 of the doxycycline washout period, Tat+ and Tat− mice were subcutaneously implanted with an ALZET® osmotic pump containing antiretroviral drug combination dolutegravir/abacavir/lamivudine (Triumeq®) with or without morphine. Mice were continuously exposed to dolutegravir, abacavir, and lamivudine ± morphine for 5 days to allow drugs to reach steady state (corresponding to day 10 of experiment). After a 5-day drug exposure, the mice were anesthetized under isoflurane and transcardially perfused with PBS. The dorsal

striatum (caudate/putamen) and hippocampus were isolated, weighed, and snap-frozen until analysis.

LC-MS/MS methods were used to quantify dolutegravir, abacavir, and lamivudine in mouse plasma and tissues. Frozen tissues were weighed, then homogenized in Precellys® hard tissue grinding kit tubes (Cayman Chemical, MI, USA) with cold 70:30 acetonitrile to 1 mM ammonium phosphate buffer (pH 7.4). Analytes were extracted from plasma and tissue homogenates following protein precipitation with the following stable isotopically labeled internal standards: abacavir-d_4, lamivudine-^{15}N-d_2, and dolutegravir-^{13}C-d_5. Chromatographic separation of analytes and internal standards from matrix components was achieved using reverse-phase chromatography on a Waters Atlantis T3 (50×2.1 mm, 3 μm) column for abacavir and lamivudine or a Waters XTERRA MS C18 (50×2.1 mm, 3.5 μm) column for dolutegravir. Analytes were detected on an AB Sciex API-5000 triple quadrupole mass spectrometer using electrospray ionization in the positive ion mode for abacavir and lamivudine or atmospheric pressure chemical ionization (APCI) in the positive ion mode for dolutegravir. The calibrated ranges for abacavir, lamivudine, and dolutegravir were 1–200 ng/mL, 0.125–50 ng/mL, and 0.025–50 ng/mL of tissue homogenate, respectively. The calibrated range for abacavir, lamivudine, and dolutegravir in plasma was 1–10,000 ng/mL, 1–4000 ng/mL, and 50–10,000 ng/mL, respectively. Precision and accuracy was ± 20% (25% at the lower limit of quantification; LLOQ). All antiretroviral data are expressed as a brain tissue-to-plasma ratio to normalize for systemic exposure.

Morphine and morphine metabolite accumulation in dorsal striatum and hippocampus

In the same mice in which antiretroviral concentrations were quantified, the contralateral brain regions were used for quantification of morphine concentrations. LC-MS/MS methods were used to quantify morphine and the major mouse glucuronidated metabolite, morphine-3-β-glucuronide (M3G). Frozen samples were weighed and thawed at ambient temperature. A 0.5 mL aliquot of water was added to each tissue or plasma sample. Each sample underwent homogenization with a micro-tissue tearor for 30 s. Following centrifugation, the sample supernatant was loaded onto preconditioned solid phase extraction cartridges (Waters HLB, Waters Corporation, Milford, MS). Samples were washed with 5% methanol and then eluted into a 96-well plate with 95% methanol (twice). Eluent was then dried under a nitrogen stream at 55 °C. Samples were then reconstituted with 0.1 mL of mobile phase prior to a 20 μL injection undergoing liquid chromatography tandem mass spectrometry (LC-MS/MS).

Morphine and its glucuronide metabolites were separated using hydrophilic interaction chromatography (HILIC) with a Polaris Silica 2.0×30 mm, 5 μm (Agilent, Santa Clara, CA, USA) HPLC column under gradient conditions. Each analyte and stable isotopic internal standard employed the following selected reaction monitoring transitions: $286.0 > 165.0$ (morphine), $462.0 > 286.0$ (M3G), $462.0 > 286.0$ morphine-6-β-glucoronide (M6G), $289.0 > 165.00$ (morphine-d3), $465.0 > 289.0$ (M3G-d3), and $465.0 > 289.0$ (M6G-d3). The linear range of the two analytes was 0.50–50 ng/mL and 1–100 ng/mL, for morphine and morphine-3-β-glucuronide, respectively. Precision and accuracy acceptance criteria were ± 15% (20% at the lower limit of quantification; LLOQ).

Western blotting

Protein expression within striatum, hippocampus, and liver (as a positive control) were analyzed by immunoblotting using standard techniques. Brain tissue samples were homogenized in lysis buffer containing protease inhibitor (Roche, Indianapolis, IN). Homogenized lysates were incubated at 4 °C for 30 min with end-over-end mixing. Liver samples were also subjected to lysis buffer containing protease inhibitor (Roche, Indianapolis, IN) but using a Precellys 24 homogenizer (Bertin Technologies, Aix-en-Provence, France) at three rounds of 10 s of bead-beating at 6000 rpm at 4 °C with ceramic beads (1.4 mm diameter, Mobio Laboratories, Carlsbad, CA). Cell debris from both brain and liver tissue samples were removed by centrifugation at 12,000 rpm for 15 min at 4 °C. Supernatants were transferred to new tubes stored at −80 °C until ready for use. Protein concentrations were quantified using the BCA protein assay (Pierce, Rockford, IL). Thirty micrograms of cell lysate was loaded on a 12% Mini-Protean TGX gel (Bio-Rad, Hercules, CA) for all proteins except for Tat− transgenic mouse liver positive control, for which 10 μg was used. Following electrophoresis and transfer to polyvinylidene difluoride (PVDF), the membrane was blocked in 5% non-fat milk solution and incubated overnight with appropriate primary antibody. Antibodies used include mouse anti-β-actin (1:4000; Sigma-Aldrich; catalog number A1978) and mouse anti-P-glycoprotein (C219; 1 μg/ml dilution; Calbiochem, Billerica, MA; catalog number 517310). Blots were then incubated at RT for 1 h with horseradish peroxidase-conjugated anti-mouse (1:20,000) secondary antibody. Signals were enhanced using chemiluminescence using the SuperSignal West Femto system (Thermo Fisher Scientific) and detected by exposure to the ChemiDoc system (Bio-Rad). The chemiluminescence signal intensity was quantified using ImageLab software (Bio-Rad). All protein expression data is expressed as relative density, which was calculated by the ratio of the absolute density of P-glycoprotein to that of β-actin absolute density.

In vivo assessment of P-glycoprotein function

The effect of morphine exposure on P-glycoprotein function was assessed by examining regional differences in the accumulation of quinidine, a P-glycoprotein substrate ± the P-glycoprotein inhibitor, PSC-833. Morphine (64 mg/mL) or vehicle (controls) was administered to mice by osmotic pump for 5 days. After 5 days of morphine or vehicle exposure, animals were administered quinidine (40 mg/kg, IP) for 1 h prior to sacrifice. To inhibit P-glycoprotein, PSC833, diluted in a mixture of Kolliphor® EL, ethanol, and saline, was administered (10 mg/kg by oral gavage) 1 h prior to quinidine administration (Kusuhara et al. 1997; Hubensack et al. 2008; Binkhathlan et al. 2010; Alhaddad et al. 2012). After sacrifice, brains were immediately harvested, weighed, and frozen at −80 °C until analysis. Quinidine concentrations were measured by LC-MS/MS (Miyata et al. 2016).

Quinidine analytical method using liquid chromatography tandem mass spectrometry (LC-MS/MS)

The determination of quinidine in mouse plasma and tissue was adapted from previously published methods (Ye et al. 2011; Achanti and Katta 2017). For LC-MS/MS analysis of plasma samples, 200 µL PBS and 25 µL of internal standard (500 ng/mL imipramine) was added to each sample and were mixed by vortex for 30 s. In order to precipitate the proteins, 250 µL of 1:1 methanol to acetonitrile with 0.2% formic acid was added to each sample and mixed by vortex for 2 min. Samples were centrifuged at 14,000 rpm (10,956 g) for 5 min, and 200 µL of the supernatant was transferred to a 1.5 mL microcentrifuge tube with a 0.45-µm filter insert (Pall Corporation, New York, USA). Samples were centrifuged a final time at 14,000 rpm (10,956 g) for 5 min to filter the supernatant. The filtered solution was transferred to 96-well plate for analysis by LC-MS/MS.

For tissue samples, striatum and hippocampus brain regions were analyzed along with plasma. Samples were thawed and centrifuged at 3000 rpm (2095 g). To each tissue sample, 200 µL of PBS was added, and the sample was then vortex mixed for 30 s. The tissue was homogenized at a gradually increasing speed for 30 s using a micro-tissue tearor, then centrifuged at 3000 rpm (2095 g) for 2 min. The supernatant was transferred to 1.5 mL microtube and 25 µL of internal standard (500 ng/mL imipramine), and 250 µL of 1:1 methanol to acetonitrile with 0.2% formic acid was added to each sample and mixed via vortex for 2 min. Samples were then centrifuged at 14,000 rpm (10,956 g) for 5 min. Two hundred microliters of the supernatant was transferred to a microfilter tube (0.45 µm) and centrifuged a final time at 14,000 rpm (10,956 g) for 5 min. The filtered solution was transferred to 96-well plate for analysis by LC-MS/MS.

Chromatographic separation was achieved using a Waters Acquity HPLC with a Zorbax SB-C18 2.1 × 50 mm 1.8 µm column (Agilent) and a gradient mobile phase (0.2% formic acid mobile phase A, acetonitrile mobile phase B). Flow was a constant 0.250 µL/mL, with 100% A from 0 to 0.5 min. From 2.5 to 3.5 min, the composition changed to 95% mobile phase B, and 50:50 mobile phase A and B from 3.6 min to 4.5 min. From 4.6 min to 5.6 min, initial conditions were re-established with 100% acetonitrile. The LC-MS/MS method employed was positive electrospray ionization and the following MRM transitions were used: quinidine (1) 325.2 > 251.1 and (2) 325.2 > 172.0 (quantification), and imipramine 281.2 > 86.1. Results were processed using Analyst 1.5.2, on an AB Sciex 4000 QTrap hybrid linear ion trap tandem mass spectrometer. The linear range for the methods was 1–5000 ng/mL as determined using a linear, 1/x regression method.

Statistical analyses

Dependent measures for BBB permeability and antiretroviral drug accumulation were assessed by two-way analyses of variance (ANOVA). Fisher's protected least significant difference *post hoc* tests determined group differences following main effects. Interactions were determined via simple main effects and main effect contrasts with error controlled for multiple comparisons. Morphine content was assessed via Student's two-tailed t tests. All comparisons were considered significant when $p < 0.05$.

Results

HIV-1 Tat and morphine independently disrupt the blood–brain barrier of mice

Following 14 days of Tat induction, there was a significant interaction with Tat and morphine for accumulation of the smallest tracer, the 10-kDa Cascade Blue®-conjugated dextran [$F(1,26) = 5.09$, $p < 0.05$]. The accumulation of 10 kDa dextran was significantly increased among Tat+ mice compared to their Tat− counterparts ($p = 0.02$; Fig. 1a). Moreover, morphine exposure significantly increased 10 kDa dextran accumulation in Tat− mouse brains, compared to those that received placebo pellets ($p = 0.047$; Fig. 1a). There was no additive effect of Tat and morphine co-exposure on dextran leakage into the brain.

With the larger tracers, significant main effects for morphine were observed. Morphine exposure significantly increased brain accumulation of the 40 kDa-labeled fluorescein-conjugated dextran [$F(1,26) = 6.19$, $p = 0.02$] (Fig. 1b), as well as the 70 kDa-labeled Texas Red®-conjugated dextran [$F(1,26) = 5.70$, $p = 0.02$], irrespective of Tat exposure (Fig. 1c).

a Cascade Blue (10 kDa)
b Fluorescein (40 kDa)
c Texas Red (70 kDa)
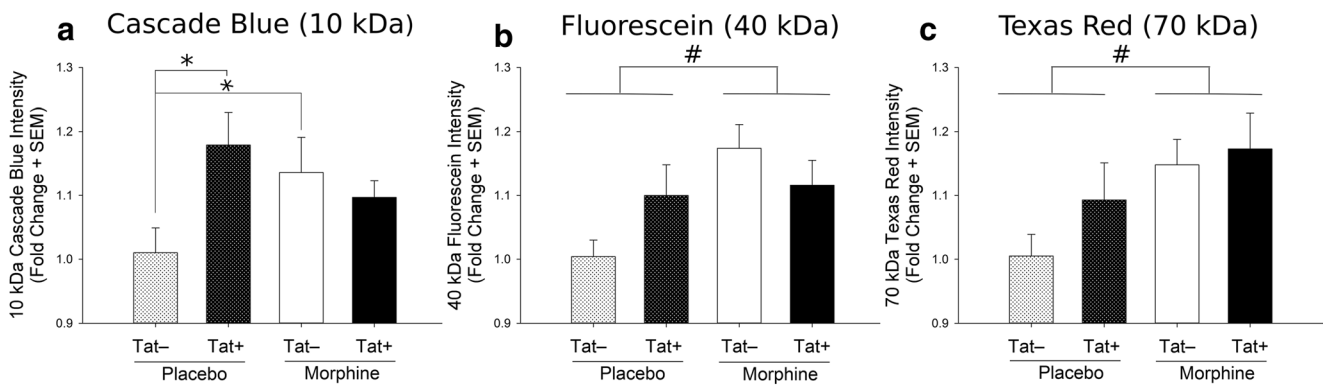
Fig. 1 Effects of HIV-1 Tat and morphine on BBB leakiness after 14-day Tat induction. There was a significant increase in the 10 kDa (Cascade Blue®) tracer leakage into the brain in Tat+ placebo as compared to Tat− placebo mice (*$p < 0.05$). The 10-kDa tracer was also significantly increased in Tat− mouse brains upon exposure to morphine as compared to Tat− placebo mice (*$p < 0.05$) (**a**). There was a significant main effect of morphine, resulting in reduced integrity of the BBB and increased leakage of the higher molecular weight (40 kDa and 70 kDa) tracers in morphine-exposed groups as compared to the those groups (Tat+ and Tat− together) not exposed to morphine (placebo) (#$p < 0.05$; significant main effect of morphine) (**b**, **c**). Data represent the fold change in mean fluorescence intensity ± SEM; $n = 8$ Tat−/placebo, $n = 6$ Tat+/placebo, $n = 9$ Tat−/morphine, and $n = 7$ Tat+/morphine mice

The negative control for the assay was fluorescence in mouse brain tissue with no exposure to dextrans. Preliminary studies demonstrated fluorescence of the negative control tissue (no dextran exposure) to be equivalent to fluorescence of Tat− placebo with transcardial infusion of dextran where the fold change in fluorescence intensity in negative control tissue was $1.017 ± 0.024$ at 380/460 nm, ex/em (Cascade Blue®-conjugated dextran, $p = 0.5386$), $1.005 ± 0.011$ at 485/520 nm, ex/em (fluorescein-conjugated dextran, $p = 0.7896$), and $1.007 ± 0.035$ at 575/620 nm, ex/em (Texas Red®-conjugated dextran, $p = 0.8907$). Additionally, the assay demonstrated a linearity of response over 40 to 400 μg/mL concentration of the dextran solution in blank brain homogenates spiked with dextrans just prior to analysis (positive control).

Effects of HIV-1 Tat and/or morphine on HRP leakiness into the striatum

At 5 min following an intracardiac injection of HRP, HRP extravasation from capillaries/post-capillary venules into the perivascular space and/or parenchyma of the striatum was evident in morphine and/or Tat-exposed mice, to a far greater extent than seen in placebo-treated Tat− (control) mice (Fig. 2). The increases of HRP leakiness confirm a previous report in the striata of Tat+ mice (Leibrand et al. 2017). Although the extent of HRP extravasation into the striatal perivascular space/parenchyma tended to appear greater with morphine than Tat exposure (arrowheads; Fig. 2b, d), a quantitative assessment is necessary to confirm this perception. Despite some variability among capillaries/venules within a single tissue section in all treatment groups, morphine and/or Tat exposure clearly increased HRP leakiness compared to Tat− controls.

Effects of HIV-1 Tat and morphine exposure on cellular/subcellular localization of ZO-1

In placebo-treated Tat− (control) mice, ZO-1 was often observed in discrete locations within endothelial cells of capillaries and venules within the striatum and hippocampus (not shown)—delineating a key aspect of the structural BBB (Fig. 3). Morphine exposure tended to cause a diffuse pattern of ZO-1 immunoreactivity within the cytoplasm of endothelial cells in Tat− mice, rather than at discrete locations associated with tight junctions as seen in placebo-treated Tat− mice (Fig. 3b). By contrast, following Tat induction, ZO-1 tended to fragment into discrete foci within the endothelium (Fig. 3c). A fragmented, rather than a diffuse distribution of ZO-1 was evident even with concurrent morphine exposure—suggesting an overriding influence of Tat on the subcellular distribution of ZO-1 (Fig. 3d). Importantly, although morphine and Tat tended to cause the diffuse or punctate patterns of ZO-1 distribution described above and shown in Fig. 3, there was some variability in the subcellular distribution of ZO-1 among adjacent microvessels within a single brain region and tissue section, suggesting the intracellular trafficking and turnover of ZO-1 is highly dynamic and perhaps dependent on highly localized differences in the CNS microenvironment. Moreover, while the striatum and hippocampus were both affected by morphine and Tat, a more systematic approach is necessary to fully appreciate the timing and nature of morphine- and Tat-dependent alterations in ZO-1 in each brain region.

Fig. 2 Effects of HIV-1 Tat and/or morphine exposure on horseradish peroxidase (HRP) extravasation from the vasculature into the perivascular space and/or parenchyma in the striatum (**a–d**). HRP antigenicity was detected by indirect immunofluorescence (*red*) in tissue sections counterstained with Hoechst 33342 (*blue*) to reveal cell nuclei and visualized by differential interference contrast (DIC)-enhanced confocal microscopy. HRP extravasation into the striatal perivascular space/parenchyma was especially prevalent in morphine-exposed mice (*arrowheads*; left-hand panels in **b** and **d**). The dotted lines (··········) indicate the approximate edge of the capillaries/post-capillary venules; while intermittent dotted lines (·· · ···) indicate the approximate edge of a partly sectioned blood vessel that appears partially outside the plane of section. The asterisks (*) indicate white matter tracts within the striatum. Representative samples from ≥ *n* = 4 mice per group. All images are the same magnification. *Scale bar* = 10 μm
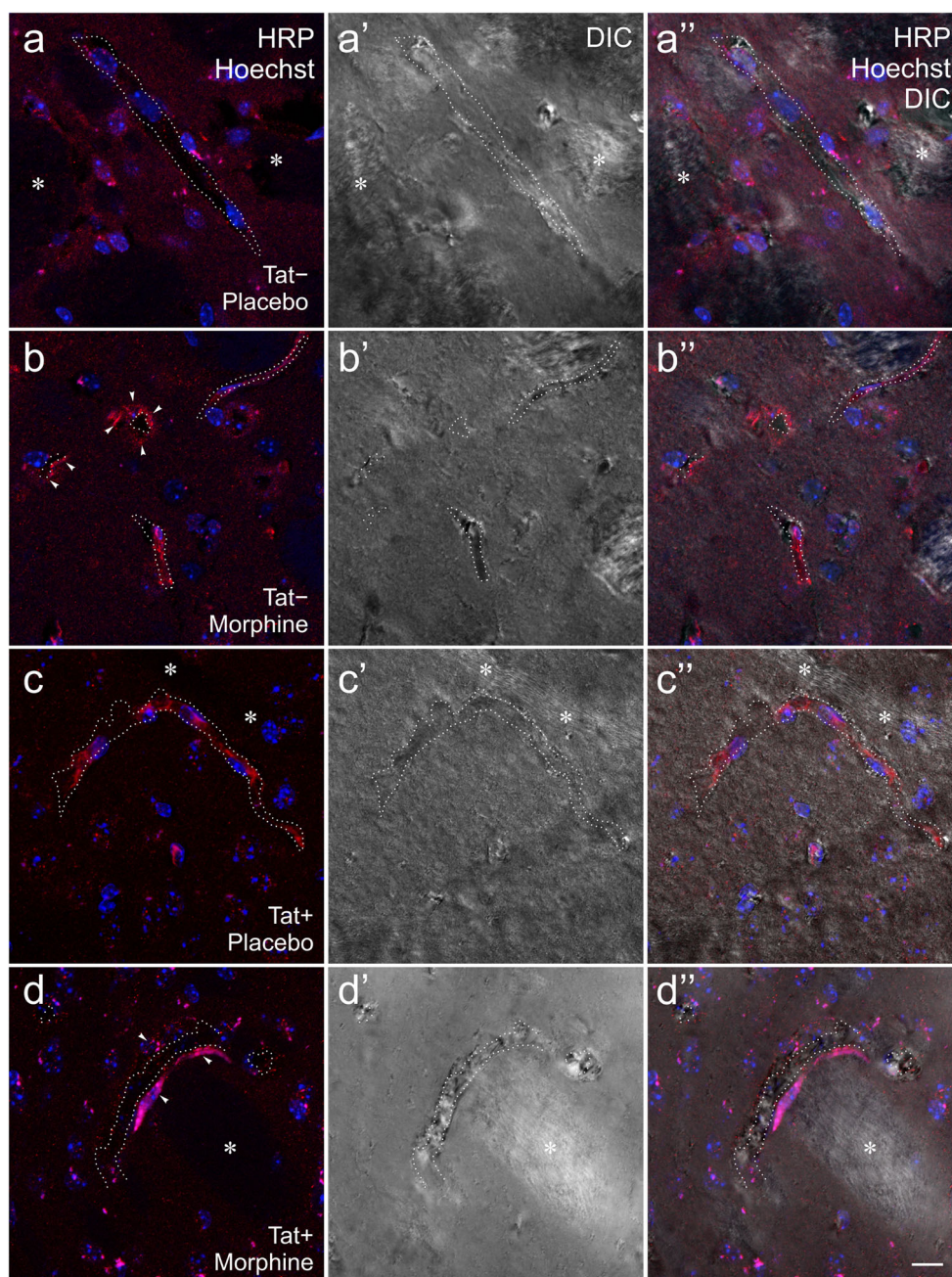
Morphine alters antiretroviral drug penetration into the brain

Morphine exposure significantly influenced antiretroviral accumulation in the brain (Fig. 4). The greatest influence was observed for morphine to significantly decrease the tissue-to-plasma ratio of dolutegravir within the striatum [$F(1,28) = 17.43$, $p = 0.0004$] (Fig. 4a) and the hippocampus [$F(1,28) = 13.80$, $p = 0.0009$] (Fig. 4d), irrespective of Tat exposure. Morphine exposure also significantly decreased the tissue-to-plasma ratio of abacavir in the striatum (but not hippocampus), irrespective of Tat exposure [$F(1,28) = 8.87$, $p = 0.007$]

(Fig. 4b). No effects were observed on the tissue-to-plasma ratio of lamivudine (Fig. 4c, f).

Tat exposure reduces morphine accumulation in hippocampus

The effects of Tat exposure on the both tissue-to-plasma ratios and raw concentrations of morphine and its M3G metabolite in plasma (Table 1), striatum, and hippocampus (Table 2) were investigated. In Tat+ mice, there was a trend towards increased morphine concentrations in plasma ($p = 0.059$) compared to their Tat− counterparts (Fig. 5a). In contrast, there was a

Fig. 3 Effects of HIV-1 Tat and/ or morphine exposure on the cellular/subcellular localization of ZO-1 immunofluorescence within the endothelial cells of capillaries and post-capillary venules in the striatum (**a–d**). ZO-1 antigenicity was detected by indirect immunofluorescence (*green*) in tissue sections counterstained with Hoechst 33342 (*blue*) to reveal cell nuclei and visualized by differential interference contrast (DIC)-enhanced confocal microscopy. Morphine exposure frequently resulted in a diffuse pattern of ZO-1 immunoreactivity within the cytoplasm of endothelial cells in Tat− mice (**b**), rather than at discrete locations associated with tight junctions as seen in placebo-treated Tat− mice (**a**). By contrast, ZO-1 tended to fragment into discrete foci within the endothelium of Tat+ mice following doxycycline induction (**c**). In the presence of Tat, ZO-1 displayed a fragmented distribution irrespective of morphine co-exposure (**d**), suggesting an overriding influence of Tat on the subcellular distribution of ZO-1. The dotted lines (··········) indicate the approximate edge of capillaries/ post-capillary venules; the intermittent dotted lines (· · · · · ·) indicate the approximate edge of a partially sectioned blood vessel. The asterisks (*) indicate white matter tracts within the striatum. Representative samples from ≥ $n = 4$ mice per group. All images are the same magnification. *Scale bar* = 10 μm
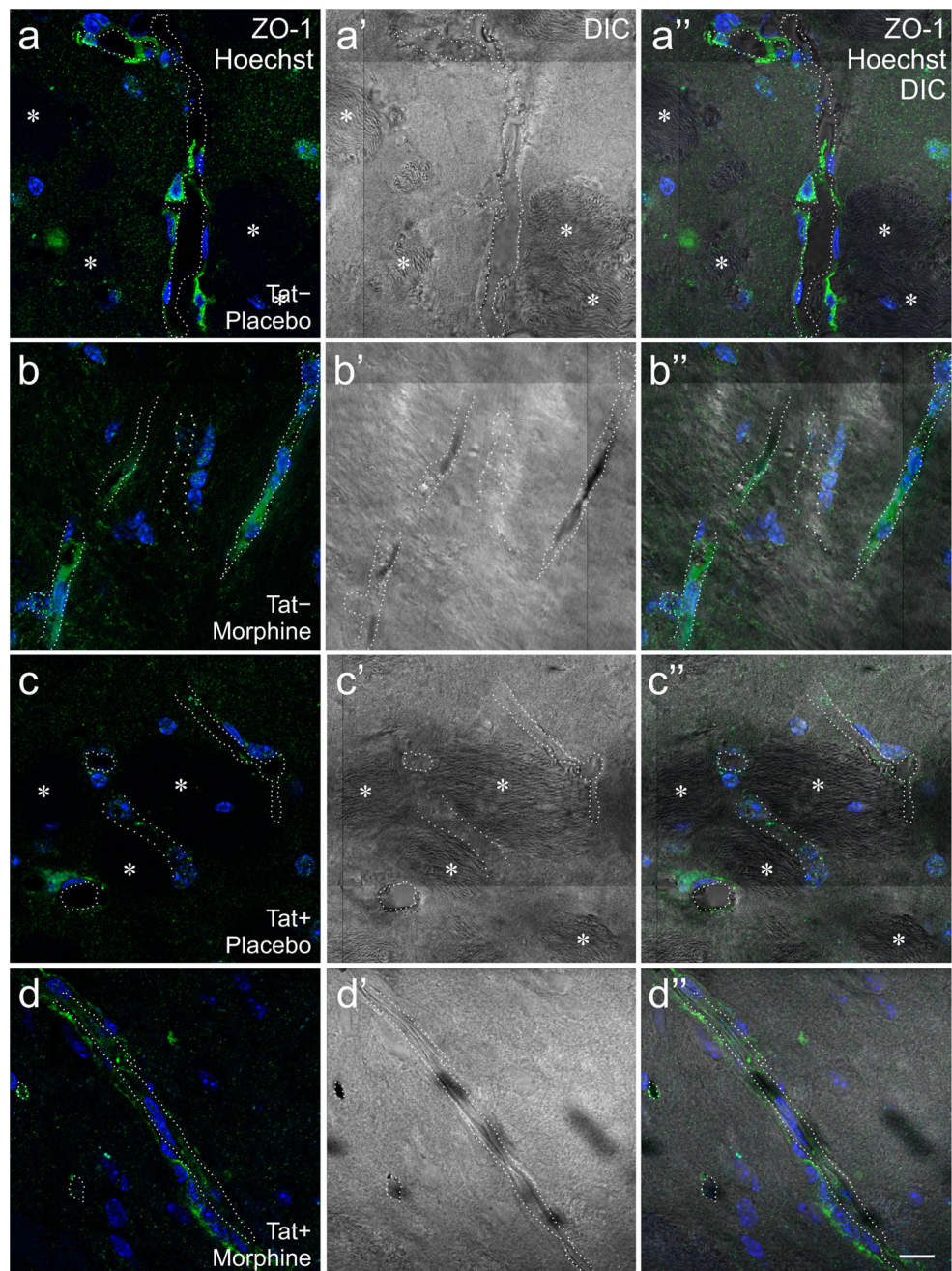

significant decrease in the tissue-to-plasma morphine ratio within the hippocampus of Tat+ ($p = 0.0499$), compared to Tat−, mice (Fig. 5c). No significant changes in morphine concentrations were noted in the striatum (Fig. 5b). There were also no significant differences in plasma M3G concentrations between Tat+ and Tat− mice (Table 1). M3G concentrations in brain tissue in Tat− mice were often below the assay's limit of quantification; only 1 of 12 Tat− brain tissue samples was quantifiable (0 in striatum and 1 in hippocampus). In Tat+ mice, 3/9 and 7/9 samples were quantified in striatum and hippocampus, respectively. Because of the limited number of quantifiable samples in brain tissue, statistical comparisons of M3G in brain tissue were not possible (Table 2).

P-glycoprotein expression and function are increased by morphine exposure

Irrespective of Tat status, exposure to morphine significantly increased P-glycoprotein expression in both striatum [$F(1,12) = 4.75$, $p = 0.0499$] (Fig. 6a, c) and hippocampus [$F(1,12) = 4.81$, $p = 0.0487$] (Fig. 6b, d) compared to placebo-treated groups. There were no significant differences
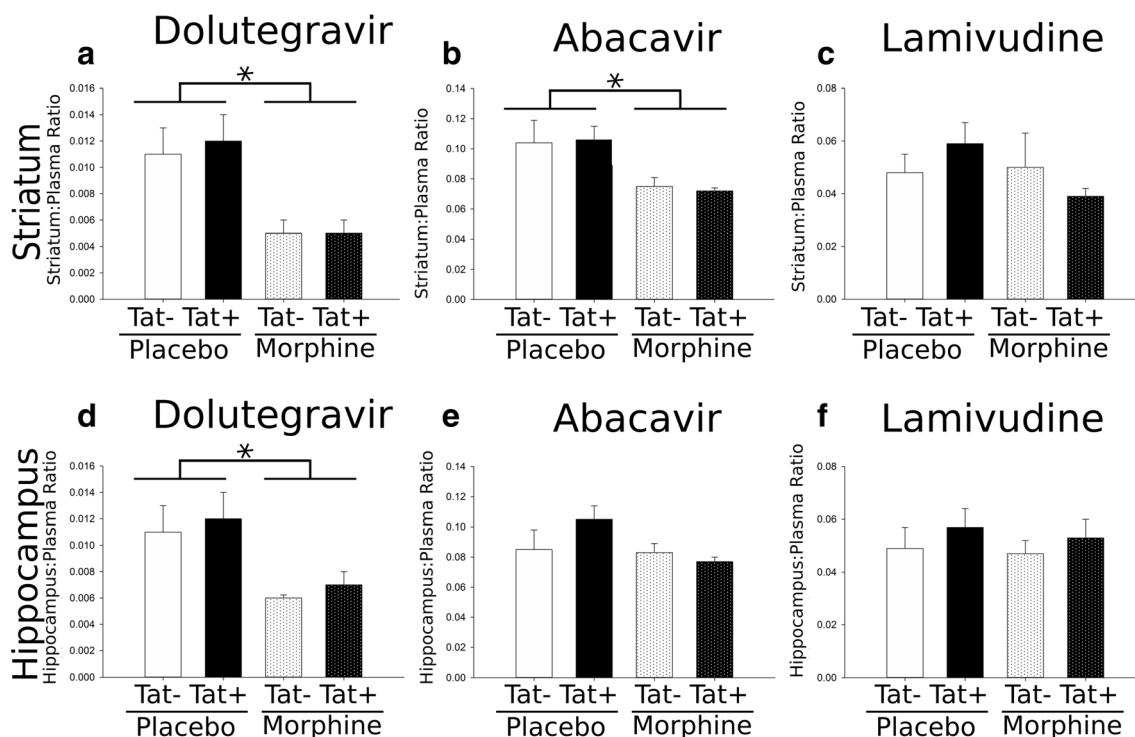
Fig. 4 Antiretroviral tissue-to-plasma ratios in striatum and hippocampus. Irrespective of Tat exposure, morphine significantly reduced the levels of striatal and hippocampal dolutegravir (**a**, **d**) and striatal abacavir (**b**), but not lamivudine (**c**, **f**), compared to placebo ($*p < 0.05$; main effect for morphine). Data represent the tissue-to-plasma ratios ± SEM sampled from $n = 9$ Tat−/placebo, $n = 9$ Tat+/placebo, $n = 6$ Tat−/morphine, and $n = 8$ Tat+/morphine mice

in basal P-glycoprotein expression levels between striatum and hippocampus in either Tat− placebo mice ($p = 0.9727$; Fig. 6e) or in Tat+ placebo mice ($p = 0.3460$; Fig. 6f) at baseline (prior to the start of treatment).

To further examine morphine's effect on P-glycoprotein, P-glycoprotein function was examined using quinidine as the P-glycoprotein substrate. Within both the striatum and hippocampus, morphine-treated mice had significantly less quinidine accumulation than the placebo-treated controls (Table 3). Furthermore, when P-glycoprotein was inhibited by pre-administration of the inhibitor PSC833, there were significant

increases in quinidine accumulation within each brain region. The accumulation ratio represents a ratio of the concentration of quinidine in the brain region with P-glycoprotein inhibition to the concentration of quinidine in the absence of P-glycoprotein inhibition. Accumulation ratios for placebo-treated striatum and hippocampus were 9.1 and 11.5, respectively, whereas in the morphine-treated groups, the accumulation ratios were 66.9 and 64, respectively, which further supports the hypothesis that morphine treatment results in increases in functional P-glycoprotein within the striatum and hippocampus.

Table 1 Raw concentrations of antiretroviral drugs, morphine and its M3G metabolite within plasma. These data are expressed as concentration (not the tissue-to-plasma ratios). Data are presented as mean ± SEM

	Plasma Drug concentration (ng/mL)			
	Placebo		Morphine	
Drug	Tat−	Tat+	Tat−	Tat+
Dolutegravir	433.2 ± 80.9	485.7 ± 60.9	634.5 ± 63.0	537.7 ± 26.2
Abacavir	1790.6 ± 607.0	1519.6 ± 184.4	1326.7 ± 84.8	1311.1 ± 62
Lamivudine	829.7 ± 320.9	500.6 ± 66.8	471.3 ± 60.2	507.8 ± 33.2
Morphine	−	−	232.1 ± 44.5	555.5 ± 122.7
M3G	−	−	2297.6 ± 369.3	2714.6 ± 279.0

Sample sizes for each experimental group was as follows: $n = 9$ Tat−/placebo, $n = 9$ Tat+/placebo, $n = 6$ Tat−/morphine, and $n = 9$ Tat+/morphine mice

Table 2 Raw concentrations of antiretroviral drugs, and morphine and its M3G metabolite within striatum and hippocampus

Drug	Striatum Drug concentration (ng/mg)				Hippocampus Drug concentration (ng/mg)			
	Placebo		Morphine		Placebo		Morphine	
	Tat−	Tat+	Tat−	Tat+	Tat−	Tat+	Tat−	Tat+
Dolutegravir	4.6 ± 1.1	5.3 ± 1.4	3.4 ± 1.0	2.4 ± 0.6	4.8 ± 1.1	5.8 ± 1.1	3.7 ± 0.4	3.7 ± 0.4
Abacavir	134.4 ± 26.1	165.8 ± 24.6	99.9 ± 10.6[†]	93.2 ± 5.9[†]	129.2 ± 26.4	163.1 ± 25.7	110.1 ± 11.5	100.2 ± 6.0
Lamivudine	25.9 ± 3.5	26.7 ± 4.9	21.5 ± 4.0	19.4 ± 1.6	27.3 ± 3.4	26.3 ± 4.5	20.8 ± 1.8	26.0 ± 3.0
Morphine			259.0 ± 107.6	322.7 ± 94.2			143.9 ± 31.1	113.2 ± 20.1
M3G			----[%]	31.6 ± 33.5[#]			21.7*	41.8 ± 12.1[^]

These data are expressed as concentration (not the tissue-to-plasma ratios). [†] $p < 0.05$; significant main effect of morphine. Data are presented as mean ± SEM Morphine-3-β-glucuronide (M3G) samples in brain tissue were often below limit of quantification (10 ng/g). The following are numbers of samples for each treatment group that were quantified for M3G; Tat+; [#] $n = 3$ (of 9), [^]$n = 7$ (of 9) and Tat−; [%] $n = 0$ (of 6), and *$n = 1$ (of 6)

Discussion

The data from these studies support four main findings. The experimental results demonstrate that (1) morphine, and to a lesser extent Tat, can result in damage to the blood–brain barrier of mice, (2) morphine exposure causes decreased penetration of select antiretroviral drugs within the brain, (3) the antiretroviral concentration changes may be caused by morphine-dependent increases in P-glycoprotein expression and function within the brain, and, finally (4) Tat exposure results in altered distribution of morphine with a tendency for higher concentrations in plasma but significantly lower plasma-normalized concentrations within the hippocampus of Tat+ mice.

Tat and morphine act independently to cause damage to BBB integrity

Our findings suggest that Tat and morphine can independently disrupt the integrity of the BBB. Tat and morphine disrupted ZO-1 expression, although perhaps through independent mechanisms (Fig. 3). Furthermore, although Tat exposure caused damage to the BBB (Figs. 1 and 2), morphine exposure resulted in more damage to the BBB, as evidenced by leakage of larger tracer molecules into the brain. Using in vitro models, others have examined the effects of Tat and morphine on tracer molecule flux across a barrier model, tight junction protein expression, and transmigration of immune cells. While some studies have demonstrated Tat and morphine exposure alters junctional protein expression (Mahajan et al. 2008; Wen et al. 2011), decreases trans-epithelial electrical resistance (TEER) (Mahajan et al. 2008), increases efflux protein expression (P-glycoprotein, multidrug resistance protein-1) (Hayashi et al. 2005, 2006; Mahajan et al. 2008), and increases transmigration (Mahajan et al. 2008), others have concluded that Tat or morphine do not increase BBB permeability through tracer leakage, nor affect P-glycoprotein within the brain (Sharma and Ali 2006; Yousif et al. 2008; Strazza et al. 2016). Our lab previously demonstrated that following Tat induction, there is a size-limited leakage of tracers into the brain; the 0.4-kDa and 44-kDa tracers freely leaked into the brain, while the larger 70-kDa tracer was excluded from entry (Leibrand et al. 2017). These findings are largely recapitulated within the current study, with additional information regarding the impact of
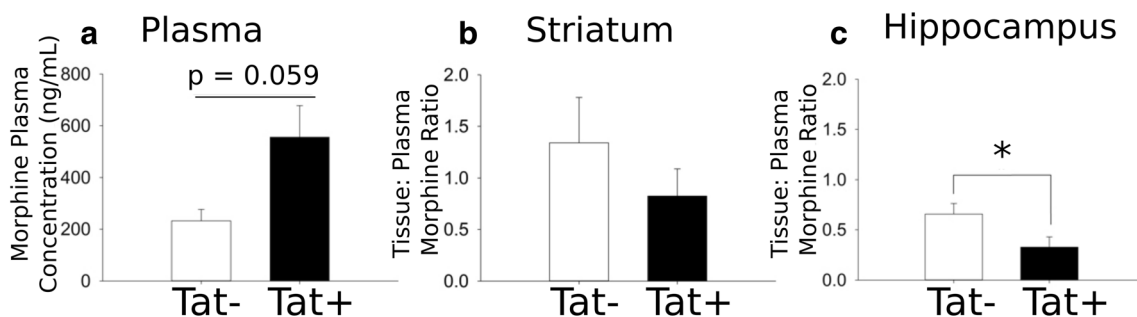
Fig. 5 Morphine plasma concentrations and tissue-to-plasma ratios in striatum and hippocampus. Morphine concentrations were measured by LC-MS/MS in both plasma and brain tissue. There was a strong trend towards significantly increased morphine plasma concentrations in Tat+ mice as compared to their Tat− counterparts (**a**). Tat exposure significantly decreased the morphine tissue-to-plasma ratio in the hippocampus (**c**) but not in the striatum (**b**) (*$p < 0.05$). Data represent the tissue-to-plasma ratios ± SEM sampled from $n = 6$ Tat−, $n = 9$ Tat+ mice
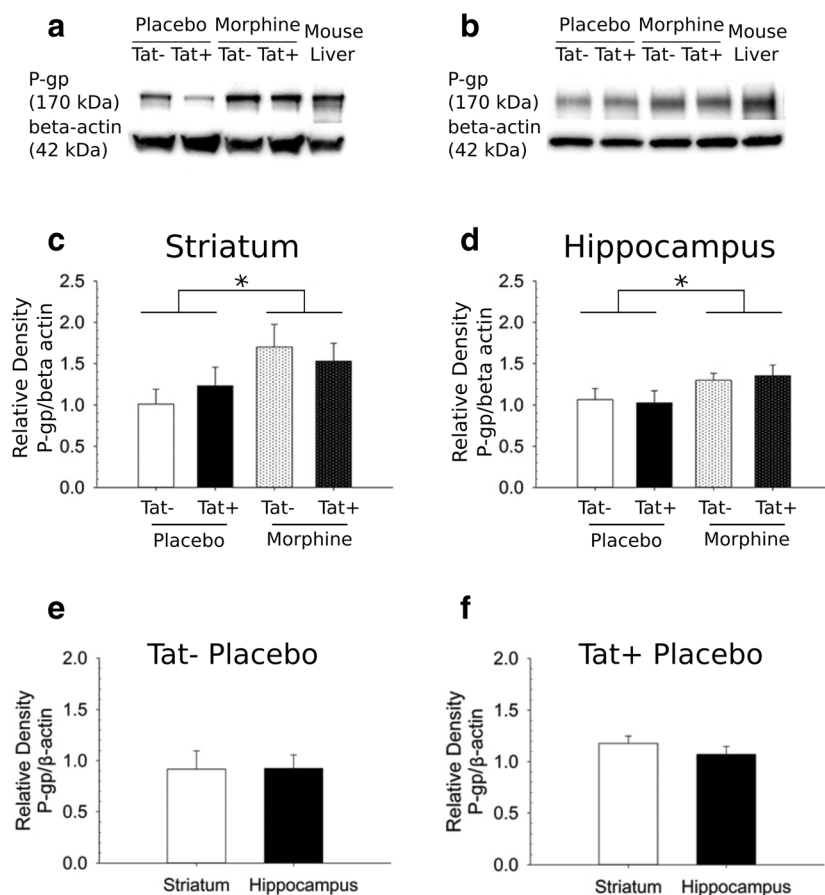
Fig. 6 P-glycoprotein (P-gp) expression levels in the striatum and hippocampus. Western blots of P-glycoprotein levels in the striatum (**a**, **c**) and hippocampus (**b**, **d**) of Tat− or Tat+ mice with or without morphine co-exposure. There was a main effect of morphine in both tissue types. Exposure to morphine, irrespective of Tat status, significantly increased P-glycoprotein expression in striatum (*$p < 0.05$; main effect of morphine) and hippocampus (*$p < 0.05$; main effect of morphine) compared with the non-morphine–exposed groups. Data represent the relative density of P-glycoprotein (absolute density of P-glycoprotein over the absolute density of β-actin) ± SEM, $n = 4$ Tat−/placebo, $n = 4$ Tat+/placebo, $n = 4$ Tat−/morphine, and $n = 4$ Tat+/morphine mice. As a negative control, baseline P-glycoprotein levels were also assessed in mice that were genetically Tat− or Tat+ but for which neither Tat induction nor morphine exposure had occurred. There were no statistically significant differences in regional expression of P-glycoprotein between striatum and hippocampus in Tat− mice or Tat+ mice at baseline (prior to Tat induction and morphine exposure; **e**, **f**). Data represent the relative density of P-glycoprotein ± SEM sampled from $n = 4$ Tat−/placebo/striatum, $n = 4$ Tat−/placebo/hippocampus, $n = 4$ Tat+/placebo/striatum, $n = 4$ Tat+/placebo/hippocampus

morphine exposure, with the exception that the intermediate sized tracer did not display significant extravasation into the brain parenchyma in Tat-exposed mice. There were some differences between the two studies. For example, the length of the Tat induction period and the introduction of a 5-day washout period before starting ARV ± morphine treatments in the current study may contribute to this discrepancy. The washout period was designed to minimize any potential pharmacokinetic drug-drug interactions between doxycycline and the antiretroviral drugs ± morphine cocktail. The specific pharmacokinetic, metabolic, and excretion profiles of each drug suggested limited potential for drug-doxycycline interactions; however, any unexpected interactions would potentially have confounded our results. Tat mRNA expression remains elevated in the striatum even after doxycycline has been removed for 4 weeks (Knapp and Xu, unpublished); therefore, it was expected that Tat levels would remain elevated over the entire study. However, we cannot rule out that some repair or recovery of the barrier may have occurred. There is also the possibility that regional differences in Tat expression levels may drive regional variation in Tat-associated increases in BBB leakiness. However, additional studies would need to be performed to confirm that Tat-associated increases in BBB leakiness are regionally selective. Regardless, the findings within this study demonstrate that morphine exposure resulted in greater breakdown of the BBB than did Tat exposure. Independent of Tat exposure, morphine promoted significant leakage of even the largest tracer (70 kDa).

Morphine exposure increased BBB leakiness but decreased ARV brain concentrations

Morphine exposure resulted in decreased ARV brain concentrations, despite increased BBB leakiness. Initially, it might

Table 3 The effects of morphine on P-glycoprotein function within the striatum and hippocampus

Tissue	Treatment	Experimental condition	Quinidine concentration (ng/g) mean ± SEM	Accumulation ratio
Striatum	Placebo	Alone	310 ± 110	9.1
	Placebo	+ P-gp inhibitor (PSC833)	2835 ± 1002*	
	Morphine	Alone	60 ± 21^	66.9
	Morphine	+ P-gp inhibitor (PSC833)	4016 ± 2315*	
Hippocampus	Placebo	Alone	290 ± 103	11.5
	Placebo	+ P-gp inhibitor (PSC833)	3345 ± 1183*	
	Morphine	Alone	69 ± 25^^	64.0
	Morphine	+ P-gp inhibitor (PSC833)	4414 ± 1561*	

Accumulation ratio is the ratio of amount of quinidine in the brain region with P-glycoprotein (P-gp) inhibition to the amount of quinidine in the absence of P-gp inhibition, for each treatment group

*Represents a significant difference between amount of quinidine in PSC833 and no PSC833 within the same treatment group, $p < 0.05$

^Comparison of quinidine concentrations within the striatum in morphine vs placebo-treated mice, $p < 0.05$

^^Comparison of quinidine concentrations within the hippocampus in morphine vs placebo-treated mice, $p < 0.05$. $n = 8$ mice for each group

seem paradoxical that morphine exposure *increases* the penetration of the dextran tracers, while *decreasing* the penetration of dolutegravir and abacavir without affecting the accumulation of lamivudine within the brain. The dextran tracers used in this study, however, traverse the BBB by passage between endothelial cells, i.e., via paracellular flux. Alterations in paracellular flux are mediated by disruption of tight junctional proteins between endothelial cells. In contrast, the overall brain penetration of the antiretroviral drugs studied herein is more likely to be influenced by mechanisms influencing passage through endothelial cells (i.e., transcellular flux). In general, drug penetration across lipid bilayers of the plasma membrane is influenced by the drug's physicochemical properties (such as lipophilicity, size, and protein binding), as well as by active transport processes. Abacavir and lamivudine entry into cells is partially mediated by passive permeability, but is also driven by the active uptake transport proteins organic cation transporters (OCT), OCT1, OCT2, and OCT3 (Yuen et al. 2008; Minuesa et al. 2009; Reis et al. 2013; Casado et al. 2014). Dolutegravir, a highly protein-bound (99%) lipophilic drug, has a high intrinsic passive membrane permeability (Reese et al. 2013) but its overall flux is also influenced by active efflux transport systems. Efflux proteins, such as P-glycoprotein, can be a major determinant to a drug's overall CNS penetration (Polli et al. 1999; Edwards et al. 2002). Although multiple uptake and efflux transporters are expressed in the mouse BBB (Miller 2010), the efflux protein, P-glycoprotein, is the only transporter for which dolutegravir and abacavir are both substrates (Shaik et al. 2007; Reese et al. 2013). Therefore, we investigated the role of morphine in influencing P-glycoprotein expression and function as a potential mechanism for the observed decreases in dolutegravir and abacavir concentrations. Increased P-glycoprotein expression within the striatum and hippocampus of morphine-exposed mice was observed (Fig. 6). In vivo functional studies

demonstrated that morphine-exposed mice also had increased P-glycoprotein activity. Mice exposed to morphine had significantly lower total tissue concentrations of quinidine (a P-glycoprotein substrate) in striatum and hippocampus as compared to the striatum and hippocampus of control mice. Furthermore, when P-glycoprotein activity was inhibited by PSC833, significant increases in quinidine concentrations in the brain were observed (Table 3). Although a role for other mechanisms, such as alterations in metabolism or other transport pathways were not examined herein, these data support the hypothesis that morphine exposure increases P-glycoprotein expression and function in striatum and hippocampus, which results in decreased tissue concentrations of P-glycoprotein substrates, such as dolutegravir and abacavir.

Other acute and/or chronic morphine exposure studies have reported increases in P-glycoprotein mRNA (Mahajan et al. 2008; Yousif et al. 2012) and protein expression within the brain and decreases in antinociceptive responses in rats (Aquilante et al. 2000; Bauer et al. 2004). However, not all studies consistently find increases in P-glycoprotein after morphine exposure (Yousif et al. 2008; Schaefer et al. 2018). In contrast to dolutegravir and abacavir, lamivudine is not a known substrate for P-glycoprotein and lamivudine concentrations in the brain were not influenced by morphine exposure. Other drug transporters, such as breast cancer resistance protein (BCRP), are also involved in the efflux of the antiretrovirals we studied. However, because P-glycoprotein is the only efflux transporter in common between dolutegravir and abacavir, a role of BCRP in mediating the observed changes in dolutegravir and abacavir concentrations in the present study is less likely (Giri et al. 2008; Kis et al. 2010; Reese et al. 2013). The implications for these findings are broad. If morphine exposure results in decreased brain concentrations of P-glycoprotein substrates, the efficacy of any CNS active, P-glycoprotein substrate drug, whether for the

treatment of HIV or any other therapeutic indication, may be reduced in patients who use opioids.

Tat altered morphine distribution within brain and plasma

Tat exposure resulted in altered morphine distribution within the plasma and brain tissue as compared to control mice. Plasma morphine concentrations in Tat+ mice were 2.4-fold higher than those in Tat− mice, although this did not reach statistical significance ($p = 0.059$). It is not clear what factors are driving this potential increase in plasma morphine concentrations, although, because there were no significant differences in M3G levels between Tat+ and Tat− mice, it does not appear to be due to changes in the rate of metabolite formation in the systemic circulation. Unlike humans, mice do not produce the bioactive M6G metabolite so alterations in the conversion morphine to M6G are not a factor. Plasma M3G concentrations were not significantly influenced by Tat status, nor was the molar morphine-to-M3G ratio within plasma significantly different between Tat+ (mean ± SEM; 0.33 ± 0.07) and Tat− (0.18 ± 0.04) mice. Morphine and M3G concentrations were also measured in striatum and hippocampus and were much lower than those observed in plasma. In the Tat− mice, only one of the 12 brain samples had M3G concentrations above the assay's lower limit of quantification (10 ng/g). For the Tat+ mice, 10 of the 18 brain samples were quantifiable, with a mean (SD) concentration of 39.76 (19.25) ng/mg tissue. This may suggest that Tat-exposed mice have higher brain concentrations of M3G but additional studies will be necessary to more fully understand Tat's influence on morphine distribution in the brain and in the plasma.

Based on regional differences in BBB structure and function at baseline, and on known regional differences in response to Tat and/or morphine (Fitting et al. 2010b), and on phenotypic variability in the responsiveness of astroglia and neurons within the same brain region (Stiene-Martin et al. 1998; Marks et al. 2016; Schier et al. 2017), it is not surprising that there would be regional differences in the effects of morphine and Tat on the concentration of antiretroviral drugs, morphine, and its M3G metabolite.

Throughout this study, total, not unbound, and antiretroviral concentrations were measured; therefore, we do not have a precise estimate of free drug within the brain. However, the focus of the present studies was to assess the directionality of effects of Tat and morphine exposure on drug concentrations. Because ARV concentrations were measured at steady state, and because we have no evidence to suggest that either Tat or morphine would cause ARV displacement from its protein binding sites, the impact on ARV tissue concentrations is expected to be proportional between total and unbound concentrations. Future studies should include measurement of intracellular total and di- and tri-phosphorylated forms of

nucleoside(tide) reverse transcriptase inhibitors (NRTIs), such as abacavir and lamivudine, to better understand whether Tat and/or morphine are affecting the activation of the NRTI drugs within cells.

Conclusions

We have demonstrated complex and regionally dependent effects of an opiate with abuse liability and HIV-1 Tat to affect CNS accumulation of antiretroviral drugs. Our findings suggest that any CNS active drug that is a P-glycoprotein substrate may be less effective in patients who are taking opioids. To more fully understand the functional impact of altered brain concentrations, future studies may include an infectious HIV model in order to assess the impact of morphine administration on antiviral efficacy.

References

Abbott NJ, Rönnbäck L, Hansson E (2006) Astrocyte-endothelial interactions at the blood-brain barrier. Nat Rev Neurosci 7:41–53

Abbott NJ, Patabendige AAK, Dolman DEM et al (2010) Structure and function of the blood-brain barrier. Neurobiol Dis 37:13–25

Achanti S, Katta RR (2017) Corrigendum to "high-throughput liquid chromatography tandem mass spectrometry method for simultaneous determination of fampridine, paroxetine, and quinidine in rat plasma: application to in vivo perfusion study" [J Food Drug Anal 24 (2016) 866-875]. J Food Drug Anal 25:1008. https://doi.org/10.1016/j.jfda.2017.01.006

Alhaddad H, Cisternino S, Declèves X et al (2012) Respiratory toxicity of buprenorphine results from the blockage of P-glycoprotein-mediated efflux of norbuprenorphine at the blood–brain barrier in mice. Crit Care Med 40:3215–3223. https://doi.org/10.1097/CCM.0b013e318265680a

Andras IE, Pu H, Deli MA et al (2003) HIV-1 Tat protein alters tight junction protein expression and distribution in cultured brain endothelial cells. J Neurosci Res 74:255–265

András IE, Pu H, Tian J et al (2005) Signaling mechanisms of HIV-1 tat-induced alterations of claudin-5 expression in brain endothelial cells. J Cereb Blood Flow Metab 25:1159–1170

Aquilante CL, Letrent SP, Pollack GM, Brouwer KL (2000) Increased brain P-glycoprotein in morphine tolerant rats. Life Sci 66:PL47–PL51

Banerjee A, Zhang X, Manda KR et al (2010) HIV proteins (gp120 and tat) and methamphetamine in oxidative stress-induced damage in the brain: potential role of the thiol antioxidant N-acetylcysteine amide. Free Radic Biol Med 48:1388–1398

Bauer B, Hartz AMS, Fricker G, Miller DS (2004) Pregnane X receptor up-regulation of P-glycoprotein expression and transport function at the blood-brain barrier. Mol Pharmacol 66:413–419

Ben-Zvi A, Lacoste B, Kur E et al (2014) Mfsd2a is critical for the formation and function of the blood-brain barrier. Nature 509:507–511

Binkhathlan Z, Hamdy DA, Brocks DR, Lavasanifar A (2010) Pharmacokinetics of PSC 833 (valspodar) in its Cremophor EL formulation in rat. Xenobiotica 40:55–61. https://doi.org/10.3109/00498250903331056

Bogulavsky JJ, Gregus AM, Kim PT-H et al (2009) Deletion of the glutamate receptor 5 subunit of kainate receptors affects the development of morphine tolerance. J Pharmacol Exp Ther 328:579–587. https://doi.org/10.1124/jpet.108.144121

Boven LA, Middel J, Verhoef J et al (2000) Monocyte infiltration is highly associated with loss of the tight junction protein zonula occludens in HIV-1-associated dementia. Neuropathol Appl Neurobiol 26:356–360. https://doi.org/10.1046/j.1365-2990.2000.00255.x

Bruce-Keller AJ, Turchan-Cholewo J, Smart EJ et al (2008) Morphine causes rapid increases in glial activation and neuronal injury in the striatum of inducible HIV-1 tat transgenic mice. Glia 56:1414–1427. https://doi.org/10.1002/glia.20708

Buckner CM, Luers AJ, Calderon TM et al (2006) Neuroimmunity and the blood-brain barrier: molecular regulation of leukocyte transmigration and viral entry into the nervous system with a focus on neuroAIDS. J NeuroImmune Pharmacol 1:160–181. https://doi.org/10.1007/s11481-006-9017-3

Buckner CM, Calderon TM, Williams DW et al (2011) Characterization of monocyte maturation/differentiation that facilitates their transmigration across the blood-brain barrier and infection by HIV: implications for NeuroAIDS. Cell Immunol 267:109–123

Casado JL, Marín A, Moreno A et al (2014) Central nervous system antiretroviral penetration and cognitive functioning in largely pretreated HIV-infected patients. J Neuro-Oncol 20:54–61. https://doi.org/10.1007/s13365-013-0228-0

Chaudhuri A, Duan F, Morsey B et al (2008a) HIV-1 activates proinflammatory and interferon-inducible genes in human brain microvascular endothelial cells: putative mechanisms of blood-brain barrier dysfunction. J Cereb Blood Flow Metab 28:697–711. https://doi.org/10.1038/sj.jcbfm.9600567

Chaudhuri A, Yang B, Gendelman HE et al (2008b) STAT1 signaling modulates HIV-1 – induced inflammatory responses and leukocyte transmigration across the blood-brain barrier. Blood 111:2062–2072. https://doi.org/10.1182/blood-2007-05-091207

Chefer VI, Shippenberg TS (2009) Augmentation of morphine-induced sensitization but reduction in morphine tolerance and reward in delta-opioid receptor knockout mice. Neuropsychopharmacology 34:887–898. https://doi.org/10.1038/npp.2008.128

Coley JS, Calderon TM, Gaskill PJ et al (2015) Dopamine increases CD14+CD16+ monocyte migration and adhesion in the context of substance abuse and HIV neuropathogenesis. PLoS One 10:e0117450

Cysique LA, Brew BJ (2009) Neuropsychological functioning and antiretroviral treatment in HIV/AIDS: a review. Neuropsychol Rev 19:169–185. https://doi.org/10.1007/s11065-009-9092-3

Dallasta LM, Pisarov LA, Esplen JE et al (1999) Blood-brain barrier tight junction disruption in human immunodeficiency virus-1 encephalitis. Am J Pathol 155:1915–1927

Dauchy S, Miller F, Couraud PO et al (2009) Expression and transcriptional regulation of ABC transporters and cytochromes P450 in hCMEC/D3 human cerebral microvascular endothelial cells. Biochem Pharmacol 77:897–909. https://doi.org/10.1016/j.bcp.2008.11.001

Dehouck MP, Méresse S, Delorme P et al (1990) An easier, reproducible, and mass-production method to study the blood-brain barrier in vitro. J Neurochem 54:1798–1801

Dohgu S, Takata F, Yamauchi A et al (2005) Brain pericytes contribute to the induction and up-regulation of blood-brain barrier functions through transforming growth factor-beta production. Brain Res 1038:208–215

Donahoe RM, Vlahov D (1998) Opiates as potential cofactors in progression of HIV-1 infections to AIDS. J Neuroimmunol 83:77–87. https://doi.org/10.1016/S0165-5728(97)00224-5

Dutta R, Roy S (2012) Mechanism(s) involved in opioid drug abuse modulation of HAND. Curr HIV Res 10:469–477. https://doi.org/10.2174/157016212802138805

Edwards JE, Brouwer KR, McNamara PJ (2002) GF120918, a P-glycoprotein modulator, increases the concentration of unbound amprenavir in the central nervous system in rats. Antimicrob Agents Chemother 46:2284–2286. https://doi.org/10.1128/AAC.46.7.2284

El-Hage N, Gurwell JA, Singh IN et al (2005) Synergistic increases in intracellular Ca^{2+}, and the release of MCP-1, RANTES, and IL-6 by astrocytes treated with opiates and HIV-1 Tat. Glia 50:91–106

El-Hage N, Wu G, Wang J et al (2006) HIV-1 Tat and opiate-induced changes in astrocytes promote chemotaxis of microglia through the expression of MCP-1 and alternative chemokines. Glia 53:132–146. https://doi.org/10.1002/glia.20262

El-Hage N, Bruce-Keller AJ, Yakovleva T et al (2008) Morphine exacerbates HIV-1 Tat-induced cytokine production in astrocytes through convergent effects on $[Ca^{2+}]_i$, NF-κB trafficking and transcription. PLoS One 3:e4093. https://doi.org/10.1371/journal.pone.0004093.t001

Ellis R, Langford D, Masliah E (2007) HIV and antiretroviral therapy in the brain: neuronal injury and repair. Nat Rev Neurosci 8:33–44

Eugenin EA (2006) CCL2/monocyte chemoattractant protein-1 mediates enhanced transmigration of human immunodeficiency virus (HIV)-infected leukocytes across the blood-brain barrier: a potential mechanism of HIV-CNS invasion and NeuroAIDS. J Neurosci 26:1098–1106

Eugenin EA, Clements JE, Zink MC, Berman JW (2011) Human immunodeficiency virus infection of human astrocytes disrupts blood-brain barrier integrity by a gap junction-dependent mechanism. J Neurosci 31:9456–9465

Fitting S, Xu R, Bull C et al (2010a) Interactive comorbidity between opioid drug abuse and HIV-1 Tat: chronic exposure augments spine loss and sublethal dendritic pathology in striatal neurons. Am J Pathol 177:1397–1410. https://doi.org/10.2353/ajpath.2010.090945

Fitting S, Zou S, Chen W et al (2010b) Regional heterogeneity and diversity in cytokine and chemokine production by astroglia: differential responses to HIV-1 Tat, gp120, and morphine revealed by multiplex analysis. J Proteome Res 9:1795–1804. https://doi.org/10.1021/pr900926n

Fitting S, Ignatowska-Jankowska BM, Bull C et al (2013) Synaptic dysfunction in the hippocampus accompanies learning and memory deficits in HIV-1 Tat transgenic mice. Biol Psychiatry 73:443–453. https://doi.org/10.1016/j.biopsych.2012.09.026.Synaptic

Fitting S, Knapp PE, Zou S et al (2014) Interactive HIV-1 Tat and morphine-induced synaptodendritic injury is triggered through focal disruptions in Na^+ influx, mitochondrial instability, and Ca^{2+} overload. J Neurosci 34:12850–12864

Fujimura RK, Goodkin K, Petito CK et al (1997) HIV-1 proviral DNA load across neuroanatomic regions of individuals with evidence for HIV-1-associated dementia. J Acquir Immune Defic Syndr Hum Retrovirol 16:146–152. https://doi.org/10.1097/00042560-199711010-00002

Gan L-S, Hsyu P-H, Pritchard JF, Thakker DR (1993) Mechanism of intestinal absorption of ranitidine and ondeansetron: transport across Caco-2 cell monolayers. Pharm Res 10:1722–1725

Gandhi N, Saiyed ZM, Napuri J et al (2010) Interactive role of human immunodeficiency virus type 1 (HIV-1) clade-specific tat protein and cocaine in blood-brain barrier dysfunction: implications for

HIV-1-associated neurocognitive disorder. J Neuro-Oncol 16:294–305

Ghazi-Khansari M, Zendehdel R, Pirali-Hamedani M, Amini M (2006) Determination of morphine in the plasma of addicts in using zeolite Y extraction following high-performance liquid chromatography. Clin Chim Acta 364:235–238. https://doi.org/10.1016/j.cccn.2005.07.002

Giri N, Shaik N, Pan G et al (2008) Investigation of the role of breast cancer resistance protein (Bcrp/Abcg2) on pharmacokinetics and central nervous system penetration of abacavir and zidovudine in the mouse. Drug Metab Dispos 36:1476–1484. https://doi.org/10.1124/dmd.108.020974.roviral

Gurwell JA, Nath A, Sun Q et al (2001) Synergistic neurotoxicity of opioids and human immunodeficiency virus-1 Tat protein in striatal neurons in vitro. Neuroscience 102:555–563

Hanamsagar R, Alter MD, Block CS et al (2017) Generation of a microglial developmental index in mice and in humans reveals a sex difference in maturation and immune reactivity. Glia 65:1504–1520. https://doi.org/10.1002/glia.23176

Hauser KF, El-Hage N, Stiene-Martin A et al (2007) HIV-1 neuropathogenesis: glial mechanisms revealed through substance abuse. J Neurochem 100:567–586

Hauser KF, Hahn YK, Adjan VV et al (2009) HIV-1 Tat and morphine have interactive effects on oligodendrocyte survival and morphology. Glia 57:194–206. https://doi.org/10.1002/glia.20746

Hawkins BT, Egleton RD (2006) Fluorescence imaging of blood-brain barrier disruption. J Neurosci Methods 151:262–267. https://doi.org/10.1016/j.jneumeth.2005.08.006

Hayashi Y, Nomura M, Yamagishi S et al (1997) Induction of various blood-brain barrier properties in non-neural endothelial cells by close apposition to co-cultured astrocytes. Glia 19:13–26

Hayashi K, Pu H, Tian J et al (2005) HIV-Tat protein induces P-glycoprotein expression in brain microvascular endothelial cells. J Neurochem 93:1231–1241. https://doi.org/10.1111/j.1471-4159.2005.03114.x

Hayashi K, Pu H, Andras IE et al (2006) HIV-TAT protein upregulates expression of multidrug resistance protein 1 in the blood-brain barrier. J Cereb Blood Flow Metab 26:1052–1065. https://doi.org/10.1038/sj.jcbfm.9600254

Hubensack M, Muller C, Hocherl P et al (2008) Effect of the ABCB1 modulators elacridar and tariquidar on the distribution of paclitaxel in nude mice. J Cancer Res Clin Oncol 134:597–607. https://doi.org/10.1007/s00432-007-0323-9

Janzer RC, Raff MC (1987) Astrocytes induce blood-brain barrier properties in endothelial cells. Nature 325:253–257. https://doi.org/10.1038/325253a0

Kanmogne GD, Kennedy RC, Grammas P (2002) HIV-1 gp120 proteins and gp160 peptides are toxic to brain endothelial cells and neurons: possible pathway for HIV entry into the brain and HIV-associated dementia. J Neuropathol Exp Neurol 61:992–1000

Kanmogne GD, Schall K, Leibhart J et al (2007) HIV-1 gp120 compromises blood-brain barrier integrity and enhances monocyte migration across blood-brain barrier: implication for viral neuropathogenesis. J Cereb Blood Flow Metab 27:123–134

Kis O, Robillard K, Chan GNY, Bendayan R (2010) The complexities of antiretroviral drug-drug interactions: role of ABC and SLC transporters. Trends Pharmacol Sci 31:22–35. https://doi.org/10.1016/j.tips.2009.10.001

Kumar R, Orsoni S, Norman L et al (2006) Chronic morphine exposure causes pronounced virus replication in cerebral compartment and accelerated onset of AIDS in SIV/SHIV-infected Indian rhesus macaques. Virology 354:192–206. https://doi.org/10.1016/j.virol.2006.06.020

Kusuhara H, Suzuki H, Terasaki T et al (1997) P-Glycoprotein mediates the efflux of quinidine across the blood-brain barrier. J Pharmacol Exp Ther 283:574–580

Leibrand CR, Paris JJ, Ghandour MS et al (2017) HIV-1 Tat disrupts blood-brain barrier integrity and increases phagocytic perivascular macrophages and microglia in the dorsal striatum of transgenic mice. Neurosci Lett 640:136–143. https://doi.org/10.1016/j.neulet.2016.12.073

Li Y, Wang X, Tian S et al (2002) Methadone enhances human immunodeficiency virus infection of human immune cells. J Infect Dis 185:118–122. https://doi.org/10.1016/j.biotechadv.2011.08.021.Secreted

Liebner S, Dijkhuizen RM, Reiss Y et al (2018) Functional morphology of the blood–brain barrier in health and disease. Acta Neuropathol 311–336. https://doi.org/10.1007/s00401-018-1815-1

Louboutin J-P, Strayer DS (2012) Blood-brain barrier abnormalities caused by HIV-1 gp120: mechanistic and therapeutic implications. Sci World J 2012:1–15. https://doi.org/10.1100/2012/482575

Louboutin J-P, Agrawal L, Reyes B a S et al (2010) HIV-1 gp120-induced injury to the blood-brain barrier: role of metalloproteinases 2 and 9 and relationship to oxidative stress. J Neuropathol Exp Neurol 69:801–816. https://doi.org/10.1097/NEN.0b013e3181e8c96f

Mahajan SD, Aalinkeel R, Sykes DE et al (2008) Tight junction regulation by morphine and HIV-1 Tat modulates blood-brain barrier permeability. J Clin Immunol 28:528–541. https://doi.org/10.1007/s10875-008-9208-1

Marks WD, Paris JJ, Schier CJ et al (2016) HIV-1 Tat causes cognitive deficits and selective loss of parvalbumin, somatostatin, and neuronal nitric oxide synthase expressing hippocampal CA1 interneuron subpopulations. J Neuro-Oncol 1–16. https://doi.org/10.1007/s13365-016-0447-2

McLane VD, Kumar S, Leeming R et al (2018) Morphine-potentiated cognitive deficits correlate to suppressed hippocampal iNOS RNA expression and an absent type 1 interferon response in LP-BM5 murine AIDS. J Neuroimmunol 319:117–129. https://doi.org/10.1016/j.jneuroim.2018.02.017

Meng J, Yu H, Ma J et al (2013) Morphine induces bacterial translocation in mice by compromising intestinal barrier function in a TLR-dependent manner. PLoS One 8:e54040

Miller DS (2010) Regulation of P-glycoprotein and other ABC drug transporters at the blood-brain barrier. Trends Pharmacol Sci 31:246–254

Miller DS, Bauer B, Hartz AMS (2008) Modulation of P-glycoprotein at the blood-brain barrier: opportunities to improve central nervous system pharmacotherapy. Pharmacol Rev 60:196–209

Minuesa G, Volk C, Molina-Arcas M et al (2009) Transport of lamivudine [(-)-beta-L-2′,3′-dideoxy-3′-thiacytidine] and high-affinity interaction of nucleoside reverse transcriptase inhibitors with human organic cation transporters 1, 2, and 3. J Pharmacol Exp Ther 329:252–261. https://doi.org/10.1124/jpet.108.146225

Miyata KI, Nakagawa Y, Kimura Y et al (2016) In vitro and in vivo evaluations of the P-glycoprotein-mediated efflux of dibenzoylhydrazines. Toxicol Appl Pharmacol 298:40–47. https://doi.org/10.1016/j.taap.2016.03.008

Nair AB, Jacob S (2016) A simple practice guide for dose conversion between animals and human. J Basic Clin Pharm 7:27–31. https://doi.org/10.4103/0976-0105.177703

Nakamuta S, Endo H, Higashi Y et al (2008) Human immunodeficiency virus type 1 gp120-mediated disruption of tight junction proteins by induction of proteasome-mediated degradation of zonula occludens-1 and -2 in human brain microvascular endothelial cells. J Neuro-Oncol 14:186–195. https://doi.org/10.1080/13550280801993630

Nath A (2015) Eradication of human immunodeficiency virus from brain reservoirs. J Neuro-Oncol 21:227–234. https://doi.org/10.1007/s13365-014-0291-1

Nath A, Hauser KF, Wojna V et al (2002) Molecular basis for interactions of HIV and drugs of abuse. J Acquir Immune Defic Syndr 31(Suppl 2):S62–S69. https://doi.org/10.1097/00126334-200210012-00006

Ngwainmbi J, De DD, Smith TH et al (2014) Effects of HIV-1 Tat on enteric neuropathogenesis. J Neurosci 34:14243–14251. https://doi.org/10.1523/JNEUROSCI.2283-14.2014

Persidsky Y, Ghorpade A, Rasmussen J et al (1999) Microglial and astrocyte chemokines regulate monocyte migration through the blood-brain barrier in human immunodeficiency virus-1 encephalitis. Am J Pathol 155:1599–1611. https://doi.org/10.1016/S0002-9440(10)65476-4

Persidsky Y, Zheng J, Miller D, Gendelman HE (2000) Mononuclear phagocytes mediate blood-brain barrier compromise and neuronal injury during HIV-1-associated dementia. J Leukoc Biol 68:413–422

Persidsky Y, Heilman D, Haorah J et al (2006) Rho-mediated regulation of tight junctions during monocyte migration across the blood-brain barrier in HIV-1 encephalitis (HIVE). Blood 107:4770–4780

Peterson PK, Sharp BM, Gekker G et al (1990) Morphine promotes the growth of HIV-1 in human peripheral blood mononuclear cell co-cultures. AIDS 4:869–873

Peterson PK, Gekker G, Schut R et al (1993) Enhancement of HIV-1 replication by opiates and cocaine: the cytokine connection. Adv Exp Med Biol 335:181–188

Peterson PK, Gekker G, Hu S et al (1994) Morphine amplifies HIV-1 expression in chronically infected promonocytes cocultured with human brain cells. J Neuroimmunol 50:167–175. https://doi.org/10.1016/0165-5728(94)90043-4

Polli JW, Jarrett JL, Studenberg SD et al (1999) Role of P-glycoprotein on the CNS disposition of amprenavir (141W94), an HIV protease inhibitor. Pharm Res 16:1206–1212

Price TO, Ercal N, Nakaoke R, Banks WA (2005) HIV-1 viral proteins gp120 and Tat induce oxidative stress in brain endothelial cells. Brain Res 1045:57–63

Pu H, Tian J, András IE et al (2005) HIV-1 Tat protein-induced alterations of ZO-1 expression are mediated by redox-regulated ERK 1/2 activation. J Cereb Blood Flow Metab 25:1325–1335

Pu H, Hayashi K, Andras IE et al (2007) Limited role of COX-2 in HIV Tat-induced alterations of tight junction protein expression and disruption of the blood-brain barrier. Brain Res 1184:333–344. https://doi.org/10.1016/j.brainres.2007.09.063

Ramirez SH, Skuba A, Fan S et al (2012) Activation of cannabinoid receptor 2 attenuates leukocyte – endothelial cell interactions and blood – brain barrier dysfunction under inflammatory conditions. J Neurosci 32:4004–4016. https://doi.org/10.1523/JNEUROSCI.4628-11.2012

Reese MJ, Savina PM, Generaux GT et al (2013) In vitro investigations into the roles of drug transporters and metabolizing enzymes in the disposition and drug interactions of dolutegravir, a HIV integrase inhibitor. Drug Metab Dispos 41:353–361. https://doi.org/10.1124/dmd.112.048918

Reis JM, Dezani AB, Pereira TM et al (2013) Lamivudine permeability study: a comparison between PAMPA, ex vivo and in situ single-pass intestinal perfusion (SPIP) in rat jejunum. Eur J Pharm Sci 48:781–789. https://doi.org/10.1016/j.ejps.2012.12.025

Sacktor N, McDermott MP, Marder K et al (2002) HIV-associated cognitive impairment before and after the advent of combination therapy. J Neuro-Oncol 8:136–142. https://doi.org/10.1080/13550280290049615

Saukkonen JJ, Furfaro S, Mahoney KM et al (1997) In vitro transendothelial migration of blood T lymphocytes from HIV-infected individuals. AIDS 11:1595–1601

Schaefer CP, Arkwright NB, Jacobs LM et al (2018) Chronic morphine exposure potentiates p-glycoprotein trafficking from nuclear reservoirs in cortical rat brain microvessels. PLoS One 13:1–16. https://doi.org/10.1371/journal.pone.0192340

Schier CJ, Marks WD, Paris JJ et al (2017) Selective vulnerability of striatal D2 versus D1 dopamine receptor-expressing medium spiny neurons in HIV-1 Tat transgenic male mice. J Neurosci 37:5758–5769. https://doi.org/10.1523/JNEUROSCI.0622-17.2017

Schwarz JM, Sholar PW, Bilbo SD (2012) Sex differences in microglial colonization of the developing rat brain. J Neurochem 120:948–963. https://doi.org/10.1111/j.1471-4159.2011.07630.x

Shaik N, Giri N, Pan G, Elmquist WF (2007) P-glycoprotein-mediated active efflux of the anti-HIV1 nucleoside abacavir limits cellular accumulation and brain distribution. Drug Metab Dispos 35:2076–2085. https://doi.org/10.1124/dmd.107.017723

Sharma HS, Ali SF (2006) Alterations in blood-brain barrier function by morphine and methamphetamine. Ann N Y Acad Sci 1074:198–224. https://doi.org/10.1196/annals.1369.020

Shiu C, Barbier E, Di Cello F et al (2007) HIV-1 gp120 as well as alcohol affect blood-brain barrier permeability and stress fiber formation: involvement of reactive oxygen species. Alcohol Clin Exp Res 31:130–137. https://doi.org/10.1111/j.1530-0277.2006.00271.x

Stiene-Martin A, Zhou R, Hauser KF (1998) Regional, developmental, and cell cycle-dependent differences in mu, delta, and kappa-opioid receptor expression among cultured mouse astrocytes. Glia 22:249–259. https://doi.org/10.1002/(SICI)1098-1136(199803)22:3<249::AID-GLIA4>3.0.CO;2-0

Strazza M, Pirrone V, Wigdahl B et al (2016) Prolonged morphine exposure induces increased firm adhesion in an in vitro model of the blood–brain barrier. Int J Mol Sci 17. https://doi.org/10.3390/ijms17060916

Tozzi V, Balestra P, Bellagamba R et al (2007) Persistence of neuropsychologic deficits despite long-term highly active antiretroviral therapy in patients with HIV-related neurocognitive impairment: prevalence and risk factors. J Acquir Immune Defic Syndr 45:174–182. https://doi.org/10.1097/QAI.0b013e318157b0f0

Troutman MD, Thakker DR (2003) Rhodamine 123 requires carrier-mediated influx for its activity as a P-glycoprotein substrate in Caco-2 cells. Pharm Res 20:1192–1199

Turchan-Cholewo J, Dimayuga FO, Gupta S et al (2009) Morphine and HIV-Tat increase microglial free radical production and oxidative stress: possible role in cytokine regulation. J Neurochem 108:202–215. https://doi.org/10.1111/j.1471-4159.2008.05756.x.Morphine

Vivithanaporn P, Gill MJ, Power C (2011) Impact of current antiretroviral therapies on neuroAIDS. Expert Rev Anti-Infect Ther 9:371–374

Weiss JM, Nath A, Major EO, Berman JW (1999) HIV-1 Tat induces monocyte chemoattractant protein-1-mediated monocyte transmigration across a model of the human blood-brain barrier and upregulates CCR5 expression on human monocytes. J Immunol 163:2953–2959

Wen H, Lu Y, Yao H, Buch S (2011) Morphine induces expression of platelet-derived growth factor in human brain microvascular endothelial cells: implication for vascular permeability. PLoS One 6:e21707. https://doi.org/10.1371/journal.pone.0021707

Wiley C, Soontornniyomkij V, Radhakrishnan L et al (1998) Distribution of brain HIV load in AIDS. Brain Pathol 8:277–284. https://doi.org/10.1111/j.1750-3639.1998.tb00153.x

Wilhelm I, Fazakas C, Krizbai IA (2011) In vitro models of the blood-brain barrier. Acta Neurobiol Exp (Wars) 71:113–128

Williams DW, Eugenin EA, Calderon TM, Berman JW (2012) Monocyte maturation, HIV susceptibility, and transmigration across the blood brain barrier are critical in HIV neuropathogenesis. J Leukoc Biol 91:401–415. https://doi.org/10.1189/jlb.0811394

Williams DW, Calderon TM, Lopez L et al (2013) Mechanisms of HIV entry into the CNS: increased sensitivity of HIV infected CD14+CD16+ monocytes to CCL2 and key roles of CCR2, JAM-A, and ALCAM in diapedesis. PLoS One 8:e69270

Williams DW, Anastos K, Morgello S, Berman JW (2015) JAM-A and ALCAM are therapeutic targets to inhibit diapedesis across the BBB of CD14+CD16+ monocytes in HIV-infected individuals. J Leukoc Biol 97:401–412

Winger RC, Koblinski JE, Kanda T et al (2014) Rapid remodeling of tight junctions during paracellular diapedesis in a human model of the blood-brain barrier. J Immunol 193:2427–2437

Wu DT, Woodman SE, Weiss JM et al (2000) Mechanisms of leukocyte trafficking into the CNS. J Neuro-Oncol 6(Suppl 1):S82–S85

Xu R, Feng X, Xie X et al (2012) HIV-1 Tat protein increases the permeability of brain endothelial cells by both inhibiting occludin expression and cleaving occludin via matrix metalloproteinase-9. Brain Res 1436:13–19

Ye Z, Tsao H, Gao H, Brummel CL (2011) Minimizing matrix effects while preserving throughput in LC-MS/MS bioanalysis. Bioanalysis 3:1587–1601. https://doi.org/10.4155/bio.11.141

Yousif S, Saubaméa B, Cisternino S et al (2008) Effect of chronic exposure to morphine on the rat blood-brain barrier: focus on the P-glycoprotein. J Neurochem 107:647–657. https://doi.org/10.1111/j.1471-4159.2008.05647.x

Yousif S, Chaves C, Potin S et al (2012) Induction of P-glycoprotein and Bcrp at the rat blood-brain barrier following a subchronic morphine treatment is mediated through NMDA/COX-2 activation. J Neurochem 123:491–503

Yuen GJ, Weller S, Pakes GE (2008) A review of the pharmacokinetics of abacavir. Clin Pharmacokinet 47:351–371. https://doi.org/10.2165/00003088-200847060-00001

Zhong Y, Smart EJ, Weksler B et al (2008) Caveolin-1 regulates human immunodeficiency virus-1 Tat-induced alterations of tight junction protein expression via modulation of the Ras signaling. J Neurosci 28:7788–7796

Zou S, Fitting S, Hahn YK et al (2011) Morphine potentiates neurodegenerative effects of HIV-1 Tat through actions at mu-opioid receptor-expressing glia. Brain 134:3613–3628. https://doi.org/10.1093/brain/awr281